Hindawi
Journal of Nanomaterials
Volume 2022, Article ID 9664365, 15 pages
https://doi.org/10.1155/2022/9664365

Research Article

Machinability Performance Investigation of TiAlN-, DLC-, and CNT-Coated Tools during Turning of Difficult-to-Cut Materials

Venkatesh Chenrayan,[1] **Chandru Manivannan**,[2] **Kiran Shahapurkar**,[1] **Ankit Krishna**,[3] **Vineet Tirth**,[4,5] **Ali Algahtani**,[4,5] **and Ibrahim M. Alarifi**[6]

[1]*Department of Mechanical Engineering, School of Mechanical, Chemical and Materials Engineering, Adama Science and Technology University, Adama 1888, Ethiopia*
[2]*Department of Mechanical Engineering, Dhirajlal Gandhi College of Technology, Salem 636309, Tamil Nadu, India*
[3]*Central Manufacturing Technology Institute, Bengaluru 560022, Karnataka, India*
[4]*Mechanical Engineering Department, College of Engineering, King Khalid University, Abha 61421, Asir, Saudi Arabia*
[5]*Research Center for Advanced Materials Science (RCAMS), King Khalid University, Guraiger, PO Box No. 9004, Abha 61413, Asir, Saudi Arabia*
[6]*Department of Mechanical and Industrial Engineering, College of Engineering, Majmaah University, Al-Majmaah, Riyadh 11952, Saudi Arabia*

Correspondence should be addressed to Ibrahim M. Alarifi; i.alarifi@mu.edu.sa

Received 4 February 2022; Revised 26 September 2022; Accepted 5 October 2022; Published 28 November 2022

Academic Editor: Zafar Iqbal

Titanium alloy-based components are now attracted by the industries with their distinguished properties even though they are difficult to machine. The tooling industries encounter numerous problems in machining these metals like higher tool wear, huge volumes of cutting fluid consumption, and shorter tool life. The objective of this research is to enhance the surface of the cutting tool with carbon nanotube (CNT) deposition to solve the aforementioned difficulties. This research used the plasma-enhanced chemical vapor deposition method to coat CNT on high-speed steel tools. Microstructural investigations were performed using a scanning electron microscope and a Raman spectroscopic technique to ensure the homogenous deposition of CNT. Additionally, scratch testing was also conducted to assess the adhesive strength of the deposited layer to the substrate. Finally, the machining performance of the CNT-coated tool was compared with commercially available diamond-like carbon (DLC) and titanium aluminum nitride (TiAlN)-coated tools. Machining experiments conducted under three distinct cutting levels revealed that the CNT-deposited tool is appropriate for turning more challenging materials. CNT-coated tools showed substantial decreases in cutting tooltip temperature, turning forces, and tool wear compared to DLC and TiAlN-coated tools. In particular, tool life studies conducted under elevated machining circumstances recorded the enhancement in tool life as 96.3% and 26.8% in comparison with TiAlN and DLC, respectively.

1. Introduction

Recently, the development and application of novel materials have been gaining popularity among the machining community. Most of these materials have hard reinforcing components and phases that greatly enhance their mechanical characteristics [1–3] but are difficult to machine, especially titanium alloys.

Liquid nitrogen and carbon dioxide have recently been employed as cryogenic coolants for machining titanium alloys. However, careless handling of these leads to snow, which could cause cold burns and persons become asphyxiated [4]. That is why more research interests today are directed toward semidry and dry machining to limit the application of different cutting fluids to retain eco-friendly environments.

However, a difficulty during the hard and dry machining process is the higher amount of heat generation at elevated temperatures, promoting the formation of built-up edges, excessive tool wear, and cutting tool failure. When machining different materials, numerous research investigations were conducted to improve the cutting efficiency and failure modes of tool with either single or multilayer-coated tools.

The wear and friction properties of these coatings were assessed in various cutting conditions [5–10].

One of the critical features of controlling the production economy is machinability. A material is considered good machining capability when it produces lesser cutting forces, negligible tool wear, and superior surface finished components with lower power consumption [11]. Therefore, the study of machinability performance is crucial and has been carried out in this work. Developing the cutting tool with minimum wear at this junction is of utmost importance to reduce tool costs over manufacturing costs by using new coating techniques.

Using the magnetron sputtering technique, titanium aluminum nitride (TiAlN) and TiN were deposited by Çalişkan et al. [12] on cold-worked 700 HV hardness tool steel. A ball on the disk set up with a load of 5 N was used for the long-distance sliding test. The tests showed that TiAlN-coated surface exhibits a lower friction coefficient when the sliding length is more, with higher wear-resistant performance than TiN coated. As a result, TiAlN coatings are best suited for applications involving high temperatures, such as hard machining. Prabakaran [13] used the physical vapor deposition method to deposit TiAlN onto a high-speed steel (HSS) tool. The results revealed that the TiAlN-coated tool had demonstrated better hardness, adhesion strength, surface quality, and wear rate than the uncoated one at various cutting speeds. Vannan et al. [14] coated the AlCrN and TiAlN bi-layer over a single-point HSS tool. The author reported that the coated tool achieved an increased tool life of 5.8 times that of the uncoated tool. In addition, the bi-layer-coated tool produced lesser wear and surface roughness than the uncoated HSS tool with the same cutting environments. Isik [11] compared the machinability of various tool steels while machining with different tools like uncoated WC, TiAlN, and (TiC/TiCN/TiN) coated inserts and HSS tool. The author reported that the most important factor affecting the tool life is cutting speed, followed by the feed rate, while cutting depth has the least impact. Aihua et al. [15] analyzed the wear and friction properties of TiAlN, AlTiN, TiN, and CrAlN coatings over cemented carbide (WC + 6% of Co) discs. They found that TiAlN and TiN coatings showed lower wear rates and superior antiwear characteristics compared to AlTiN and CrAlN coatings.

Diamond-like carbon (DLC) coatings receive greater interest because of their extreme hardness, lower thermal expansion, and good lubricity properties. Hence, the contribution of DLC in numerous applications is much more prevalent in recent days [16]. The DLC coatings obtained by the plasma-enhanced chemical vapor deposition (PECVD) technique contain a considerable volume of hydrogen (40–60 at%); hence, they are usually identified as simply a-C:H or hydrogenated amorphous DLC coatings. They typically have a combination of metastable sp^2 and up to 70% of sp^3 carbon bonding of a high fraction [17, 18].

A few researchers noted the poor adherence of DLC coating with the substrates who tested them on various workpiece materials and cutting processes [19–21]. Dos Santos et al. [22] experimented to evaluate the machining forces during the turning of Al–Si alloys (12 and 16 wt% of Si) with DLC-coated-cemented carbide inserts. The author observed that DLC-coated tools lead to a reduction in feeding forces when turning Al–Si alloys. Folea et al. [23] investigated the performance of DLC-coated cutting tools under different cutting conditions on various workpiece materials. The authors found that while machining aluminum alloys and composites, DLC-coated tools exhibit improved surface roughness, reduction in wear and cutting forces. In some situations, composite coatings are more beneficial than single-layer coatings as they give their constituents combined unique properties. Wada et al. [24] examined the surface roughness and tool wear of three different cutting tools coated with DLC, DLC/(Al, Cr) N, and uncoated HSS tools for turning Al–Si alloys. The author found that DLC with an interlayer of Cr-based tool showed lesser wear progression than DLC-coated tool and produced a constant surface roughness for a particular cutting length.

Carbon-based materials are often regarded as the most promising candidates in the advancement of nanotechnology. Carbon nanotubes (CNTs) are carbon molecules in cylindrical shape formed by the rolling up of graphene sheets (single-layer carbon atoms). The structure of CNT consists of strong molecular interaction of sp^2 bonds [25]. The thermal and mechanical properties of hollow glass microspheres-reinforced epoxy composite have been improved by using CNTs and graphene nanofillers [26]. Recently, the use of CNTs is of vital importance in developing hard surface coatings owing to their excellent shear and tensile strength, self-lubricating property, high thermal conduction, wear proof, and low friction coefficient [27, 28]. The unique characteristics of CNTs make the work materials superior in surface finish and significantly reduce tool wear. Pazhanivel et al. [29] examined the machinability and wear behavior of CNT-deposited cutting inserts. The results revealed that inserts coated with multiwalled carbon nanotubes (MWCNTs) exhibited improved machinability with an excellent surface finish due to their negligible friction coefficient. The sliding friction properties of CNTs were analyzed by Hirata and Yoshioka [30] by coating CNTs over cemented carbide, silicon nitride, and silicon substrates. The test results explored improved lubrication and greater adhesive strength of CNTs while coated over the porosity substrates. Borkar and Harimkar [31] reported that the pulse electrodeposition of CNTs-reinforced composite coating significantly improved wear resistance compared with pure nickel coating.

The mechanical characteristics of single and MWCNTs have been studied by Salvetat et al. [32]. The author stated that the structure of nanotubes strongly impacts mechanical properties due to the high degree of graphite anisotropy. Small single-walled carbon nanotubes (SWCNTs) have a higher value of Young's modulus than graphite. Young's modulus value of CNT coating is over 1 TPa [25, 33], which is well above 100–300 GPa of DLC [18]. Several authors researched CNT coatings on various substrates to increase thermal, mechanical, and anticorrosive qualities [34–36]. Abdulrahaman et al. [36] explored the corrosion, and the mechanical characteristics of CNT deposited on mild steel

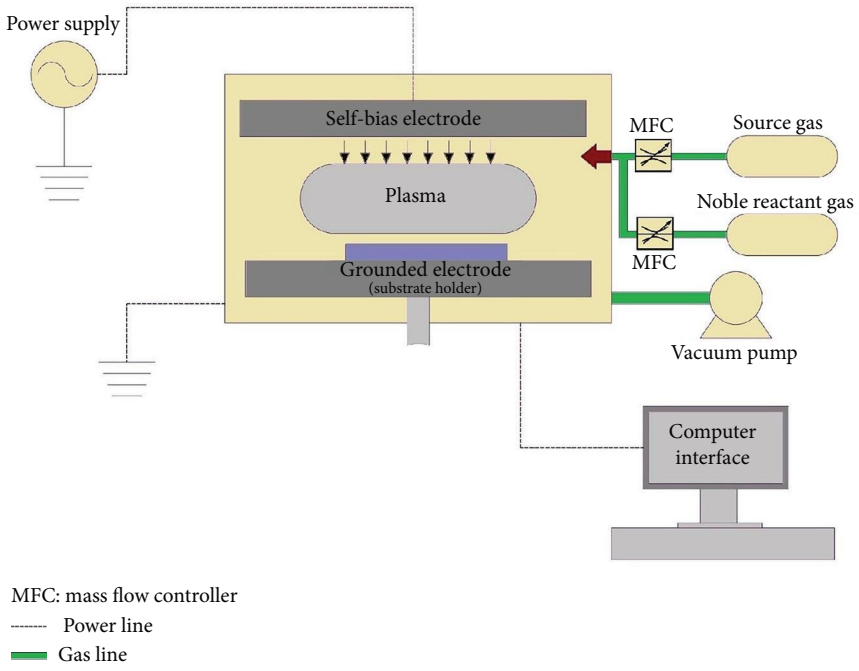

Figure 1: Schematic diagram of PECVD process.

by varying test parameters such as coating temperature and holding period. The authors observed that increasing the holding time and coating temperature improves the yield strength, hardness, and tensile strength of the CNT-coated samples and decreases corrosion rate.

Most current research literatures focus on carbide tools as substrates, primarily coated with chromium and titanium composite components. Very few existing literatures deal with carbide tools as a substrate and coated by MWCNT. In this research work, the novel SWCNTs were deposited over widely utilizing HSS cutting tools by the PECVD technique. No other previous study has ever been reported regarding CNT deposition on HSS tools, and subsequently performance analysis by considering all machining characteristics in a single effort. The extensive study of the performance of a CNT-coated tool by including the maximum possible four machining objectives when turning titanium alloy, a low machinability material [37, 38], highlights the novelty and originality part involved in the work.

2. Materials and Methods

2.1. Deposition of CNT. CNT deposition was accomplished using PECVD equipment from Roth and Rau microsystems, Germany, whose schematic representation is illustrated in Figure 1. Initially, AISI M2 high-speed steel (4 inch length and 1/2 inch width) substrates had been thoroughly cleaned for ~20 min using an ultrasonic cleaner to remove dust, dirt, and soil particles present over the surfaces. A thin nickel layer was introduced over the HSS substrates by the direct current sputtering method before CNTs were coated. It serves as a good catalyst for CNT growth. A gaseous mixture of acetylene and hydrogen with the ratio of 1 : 8 was used in the PECVD apparatus to grow SWCNTs. Typically, the reaction chamber is excited at a frequency of 2.45 GHz to generate plasma. Plasma microwave stimulates the supply of hydrocarbons and breaks off molecular hydrogen. Electrons oscillate as a result of the plasma energy, colliding with gas atoms and molecules to produce ions. Table 1 summarizes the deposition parameters used in the experiment.

Table 1: Deposition parameters.

Flow rate of acetylene	3 cc/min
Flow rate of hydrogen	20 cc/min
Chamber pressure	2.5×10^{-2} mbar
Microwave power	200 W
Bias voltage	550 V (on self-bias mode)
Deposition time	40–45 min

2.2. Scratch Test. A Raman spectrometer was used to acquire micro-Raman spectra of SWCNTs coated on the substrate under backscatter geometry of 532 nm wavelengths. The morphology of CNT coating was investigated using a SUPRA 55VP field emission scanning electron microscope (SEM) from Carl Zeiss. A microscratch test as per ASTM C1624 standard has been conducted for the coating conformity evaluation. It was carried out by a DUCOM scratch wear tester, in which a 200 μm radius rounded tip Rockwell diamond indenter was used to scratch the workpiece. The samples are subjected to a ramp load of 20 N at the beginning and 45 N at the end in a progressively rising order with 0.2 mm/s constant scratch speed for 6 mm

Table 2: Chemical constitution of titanium grade 5 alloy.

Chemical components	O	N	V	H	Fe	Al	C	Ti
Percentage	0.20	0.05	3.50–4.50	0.0125	0.40	5.50–6.75	0.10	Remaining

Table 3: Mechanical characteristics of titanium grade 5 alloy.

Hardness	Yield strength	Tensile strength	Elongation	Reduction in area
36 HRC	900 MPa	895 MPa	10%	25%

Table 4: Experimental setup technical specifications.

Description	Unit	Size
CNC system and model	–	FANUC Series 0i Mate TD
Number of turret stations	–	8
Number of axis	–	Two (z and x)
Max. travel in z-axis	mm	400
Max. travel in x-axis	mm	140
Between center length	mm	425
Standard spindle speed	rpm	3,000
Max. length of turning	mm	400
Max. diameter of turning	mm	270

stroke length. The test was continued until failure occurred at the critical load. An optical microscope was used to determine the breadth of the scratched track.

2.3. Turning Experiments. Commercial grade 5 titanium alloy was used as a working material for machining experiments. Its chemical constitution and mechanical characteristics are represented in Tables 2 and 3, respectively.

The turning experiments were conducted in an ACE Micromatic CNC lathe (Model: Jobber LM) to turn the titanium grade 5 alloy, specified in Table 4. The machining parameters chosen for the experiments are listed in Table 5. Three different coated HSS tools, namely CNT, DLC, and TiAlN HSS tools were employed for machining experiments under dry cutting conditions. DLC was deposited over the HSS tools similar to CNT deposition as briefed earlier. TiAlN films were deposited on HSS tools using a magnetron sputtering system.

2.4. Measurement of Cutting Temperature. The cutting tool's performance is significantly influenced by the cutting temperature at the tooltip and workpiece interface. The thermal image camera FLIR E50 was used for temperature measurement in the cutting zone while turning 50 mm diameter and 150 mm length titanium alloy. The thermal imaging camera has an automotive orientation system, a resolution of 3.1 MP, an IR resolution of 240×180, a 60 Hz frame refresh, and a thermal sensitivity of 0.05°C. It can record a minimum of −20°C to a maximum of 1,000°C and is fixed onto a special device, as illustrated in Figure 2. The constant proximity of contact has been ensured by setting precise angles and heights with the adjustments available in the setup.

Table 5: Experimental machining parameters.

Level/ parameter	Speed of cutting (m/min)	Cutting depth (mm)	Rate of feed (mm/rev)
Level 1	250	0.3	0.20
Level 2	350	0.5	0.25
Level 3	450	0.8	0.30

2.5. Measurement of Cutting Forces. Cutting forces are intrinsic phenomena and an important measuring index of cutting performance. The cutting forces developed over three different tools under the three levels of cuts were measured with the help of a KISTLER dynamometer (type 5697A) and a DyanoWare data acquisition program. It was carried out by maintaining a cutting time of 60 s for each experiment.

2.6. Measurement of Tool Wear. The lifetime of the cutting tool is influenced significantly by its wear behavior. A high-quality NT-MDT (model: NTEGRA) atomic force microscope (AFM) and a Dino-Lite digital microscope with an image resolution of 640×480 megapixels, a magnification range of 10× to 230×, and a video frame rate of 30 FPS were used to test the wear progression under all the cutting circumstances.

2.7. Measurement of Chip Morphology. Chip morphology is an essential technique to validate the machining objectives concerning the level of machining parameters. The appearance, color, and nature of the chips are beneficial to study the tribological interaction between tool/workpiece regions. The metal chips were obtained at determined intervals during each level of the machining condition, and a high-resolution digital camera was employed to capture their images. The images were examined to determine the effect of machining factors on the machining objectives related to the tool surface and tribology effect.

3. Results and Discussion

3.1. Characterization of CNT Deposition. A sample Raman spectrum of the SWCNTs with their peak characteristics is shown in Figure 3. Raman's radial breathing mode (RBM) feature observes the atomic vibrations of the C atoms in the radial direction when the CNT was breathing during the deposition process. The RBM shown in Figure 3 confirms the existence of SWCNT. Besides, the multipoint tangential G band around 1582 cm^{-1} also validates the sound signature

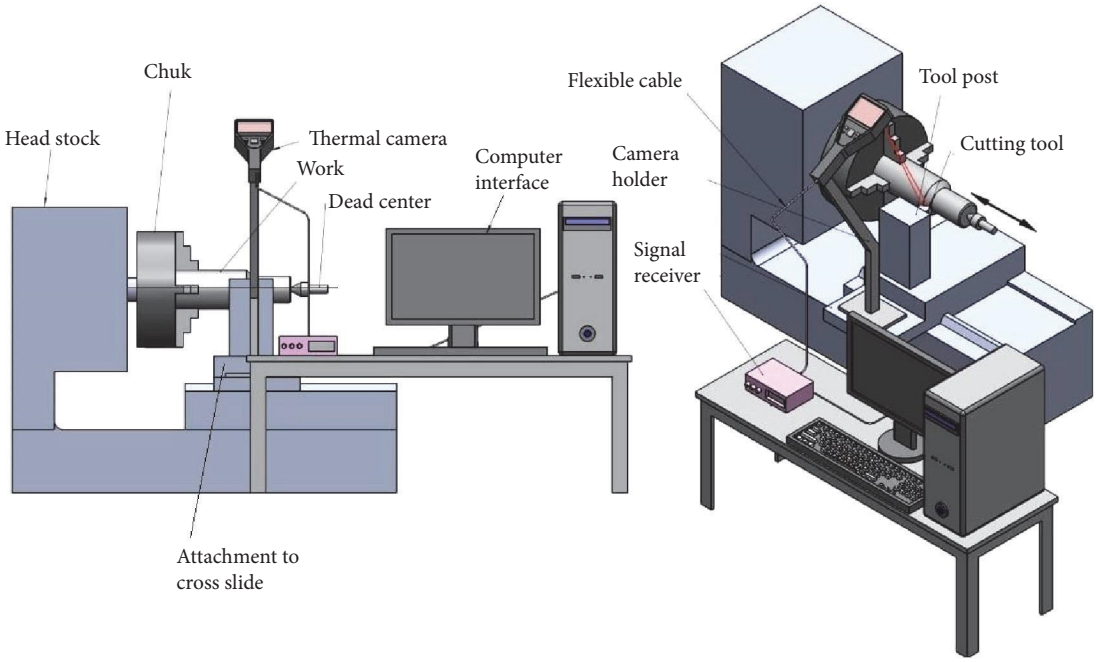

Figure 2: Schematic arrangement of the infrared thermal image camera.

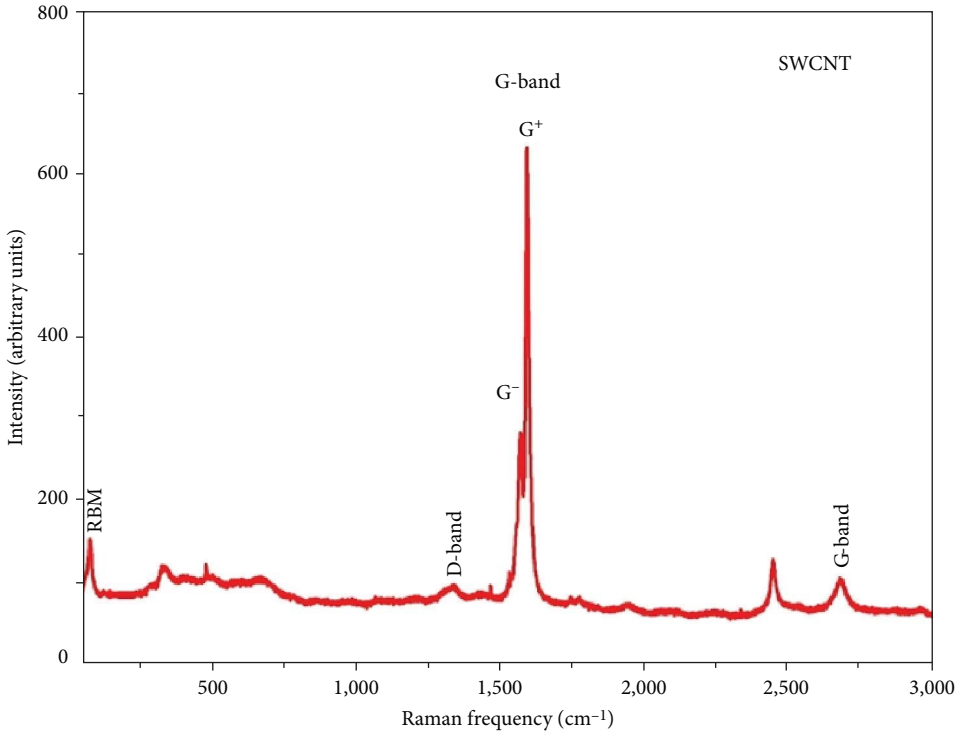

Figure 3: Raman spectra of SWCNT.

of the SWCNT. In SWCNT, the tangential G mode bands produce multipeak features known as G^+ and G^- represent the atomic displacement along the tube axis and the circumferential direction, respectively, and the nanotube curvature causes the lowering frequency of the G^- mode. Moreover, the D-band signal with a low-intensity frequency of about 1,350 cm^{-1} indicates the good structural quality of SWCNT used in this study [39].

Figure 4 shows SEM images of CNT deposition, in which perfect images of coated CNTs with lower aspect ratios were observed. SEM images also ensure dense deposition of CNTs. Fellow researchers [40] have attempted to investigate the

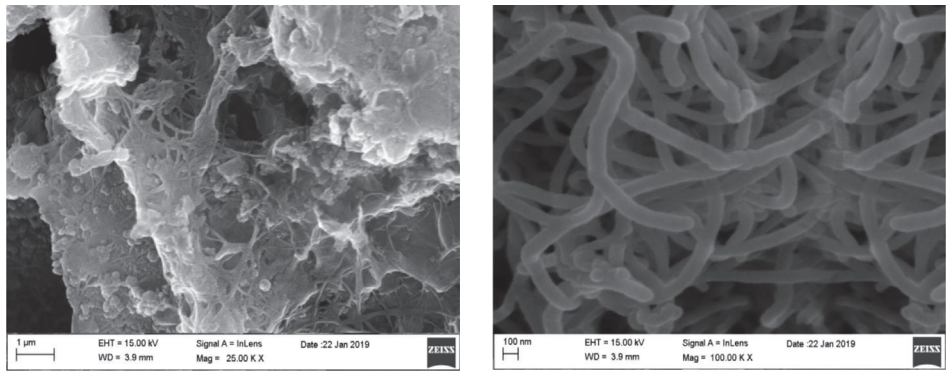

Figure 4: Micrograph of CNT deposition.

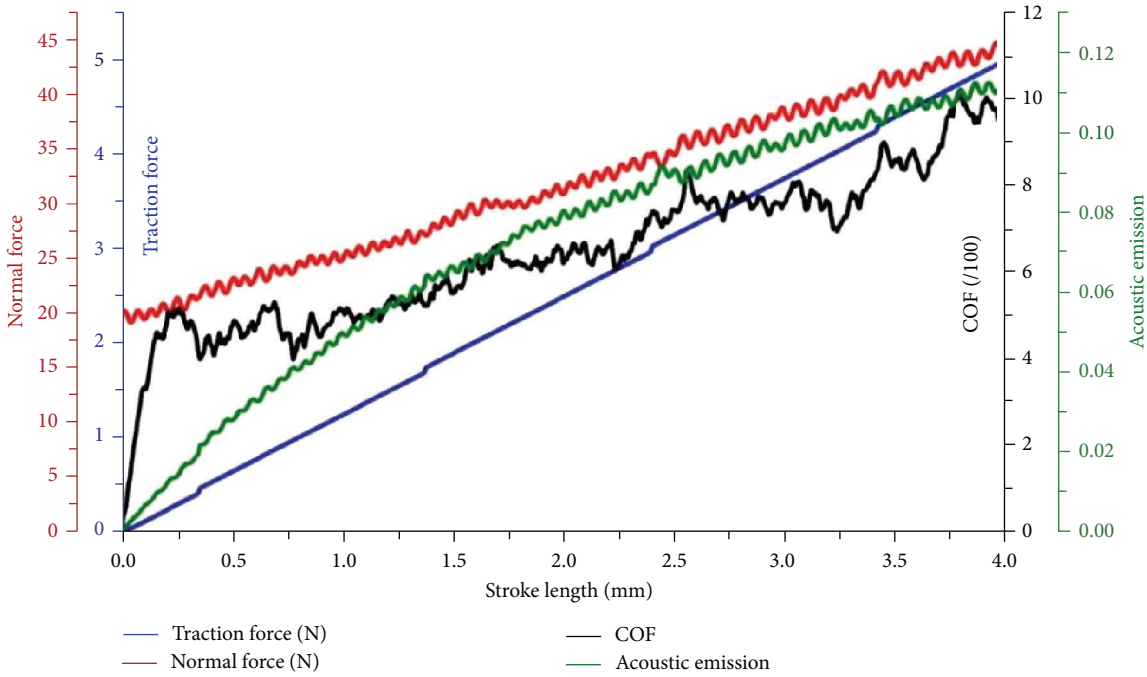

Figure 5: Scratch test data plot.

weak adherence of CNT coatings to the substrate, one of which has observed that if the CNT are longer in length, they can be peeled off from the substratum. The aspect ratio (length/diameter) of a CNT is a decisive factor in the adherence to the substratum. The coating adherence to the substratum is inversely proportional to the aspect ratio of CNTs; thus, for greater adherence, the CNT should have a smaller aspect ratio [29]. The microwave power of CVD can be controlled in a decreased way to grow shorter CNT [30].

3.2. Adhesive Strength of the CNT Deposition. The tangential frictional force and acoustic emission are used to quantify the output. Surface scratching causes increased elastic and plastic deformations until the coating spalls significantly from the substrate material at the critical load, W_c. Figure 5 shows the scratch test results with four different lines. The black line expresses the friction coefficient; the green line indicates the acoustic emission. The remaining two lines, blue and red, are the traction force and normal load, respectively.

The average friction coefficient value between the CNT film and the HSS substrate was found to be 0.075. Hirata and Yoshioka [30] reported that the average CNT deposition friction coefficient is 0.1 on W_c inserts. The width of the scratch track was measured as 123 μm using an optical microscope, as shown in Figure 6.

Equation (1) gives an empirical relationship for determining the adhesive strength of the coating to the substrate material [41].

$$\sigma_A = \frac{2W_c}{\pi R b}, \tag{1}$$

where σ_A: adhesion strength (N/mm^2), R: stylus tip radius (mm): 0.2 mm, W_c: observed critical load (N): 26 N, b: breadth of the scratched track produced due to W_c (mm): 123 μm.

The adhesion strength computed by the above relationship is 673 N/mm^2, about 3/4th of its yield strength value of 900 N/mm^2.

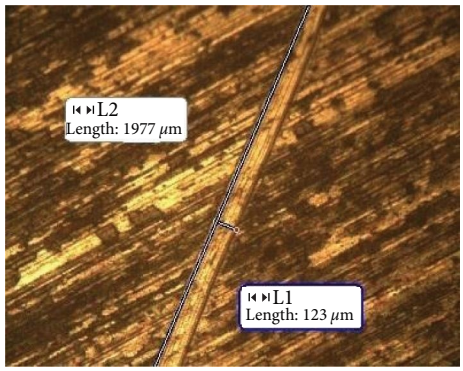

Figure 6: Microscopic image of the scratch track.

3.3. Cutting Tooltip Temperature. Figure 7 shows the sample observations obtained from the thermal image camera during the machining of the workpieces with TiAlN, DLC, and CNT-coated tools at Level 2 cutting conditions. The yellow color zone represents the maximum temperature, while the blue color zone is the lowest. The maximum temperatures measured for the TiAlN, DLC, and CNT-coated tools are 349.4, 174.8, and 115.5°C, respectively, as shown in Figure 7.

The comparative temperature results for the uniform cutting duration of 15 min under all the machining conditions are given in Figure 8. The results demonstrate that the cutting tooltip temperature rises as the cutting speed increases for all the tools. The graphs indicate that the temperature of the CNT-coated tooltip was around 67% lower than that of the TiAlN-coated tooltip and 36% lower than that of the DLC-coated tooltip under Level 1 cutting conditions. Under Level 2 circumstances, the results indicate that the CNT-coated tooltip registered a temperature about 67% lower than the TiAlN-coated tool and 34% lower than the DLC-coated tool. Compared to TiAlN and DLC, the CNT-coated cutting tool exhibited about 71% and 33% decrease in the cutting temperature at Level 3, respectively. It is, therefore, quite obvious that among the three coated tools, TiAlN-coated tool has recorded the highest cutting temperature, followed by DLC-coated tool, and CNT-coated tool recorded the least temperature compared to TiAlN and DLC-coated tools in all cutting situations.

The contact between the tooltip and workpiece normally results in higher friction, which leads to heat development. The higher value of friction coefficient of TiAlN coating of 0.6 [42] results in more heat generation during machining, whereas the coefficient of friction of DLC-coated tool is 0.17–0.25, according to the previous research reports [43, 44]. However, the scratch test showed that the CNT-deposited surface has an excellent lubricating property with an extremely low friction coefficient of 0.075. This remarkably meager value of coefficient of friction of CNT tool paves the way to record a lesser temperature, lesser the value of coefficient of friction lesser the chip-tool abrasion, which in turn minimizes the cutting tool temperature.

Another reason with which the CNT-deposited tool records lesser cutting temperature is its unique thermal conductivity. There would be a significant increase in thermal

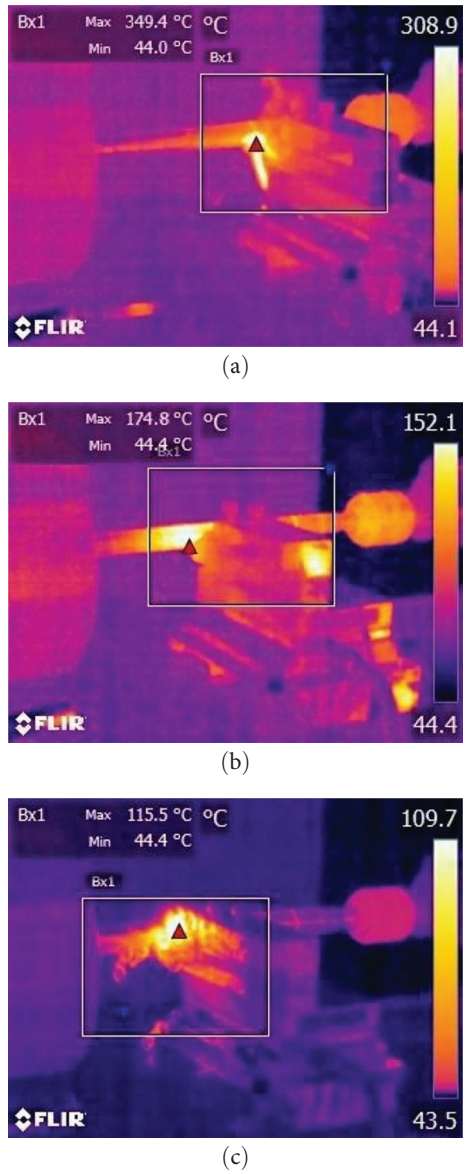

Figure 7: Infrared images acquired while machining with (a) TiAlN; (b) DLC; (c) CNT-coated tools under Level 2 cutting condition.

conductivity for very low sp^2 structure contents and the order of its phase in graphite regions [45]. As CNT is made up of a large amount of low sp^2 bonds, its thermal conductivity is around 6,000 W/m K [25, 46], which is much higher than that of DLC as 0.566 W/m K [45] and TiAlN as 50 W/m K [47]. This noble characteristic of CNT helps the chips to drain the majority of the heat produced at the tool-workpiece interface to the atmosphere. Thus, the combined effect of high lubricative surface and excellent thermal conductivity of the CNT-deposited tool dramatically reduces the tooltip temperature.

3.4. Cutting Forces. Machinability is significantly affected by the cutting forces produced by the tool during machining. Figure 9 illustrates the comparative cutting force results for TiAlN, DLC, and CNT-coated cutting tools in the three different cutting conditions. The graphs confirmed that

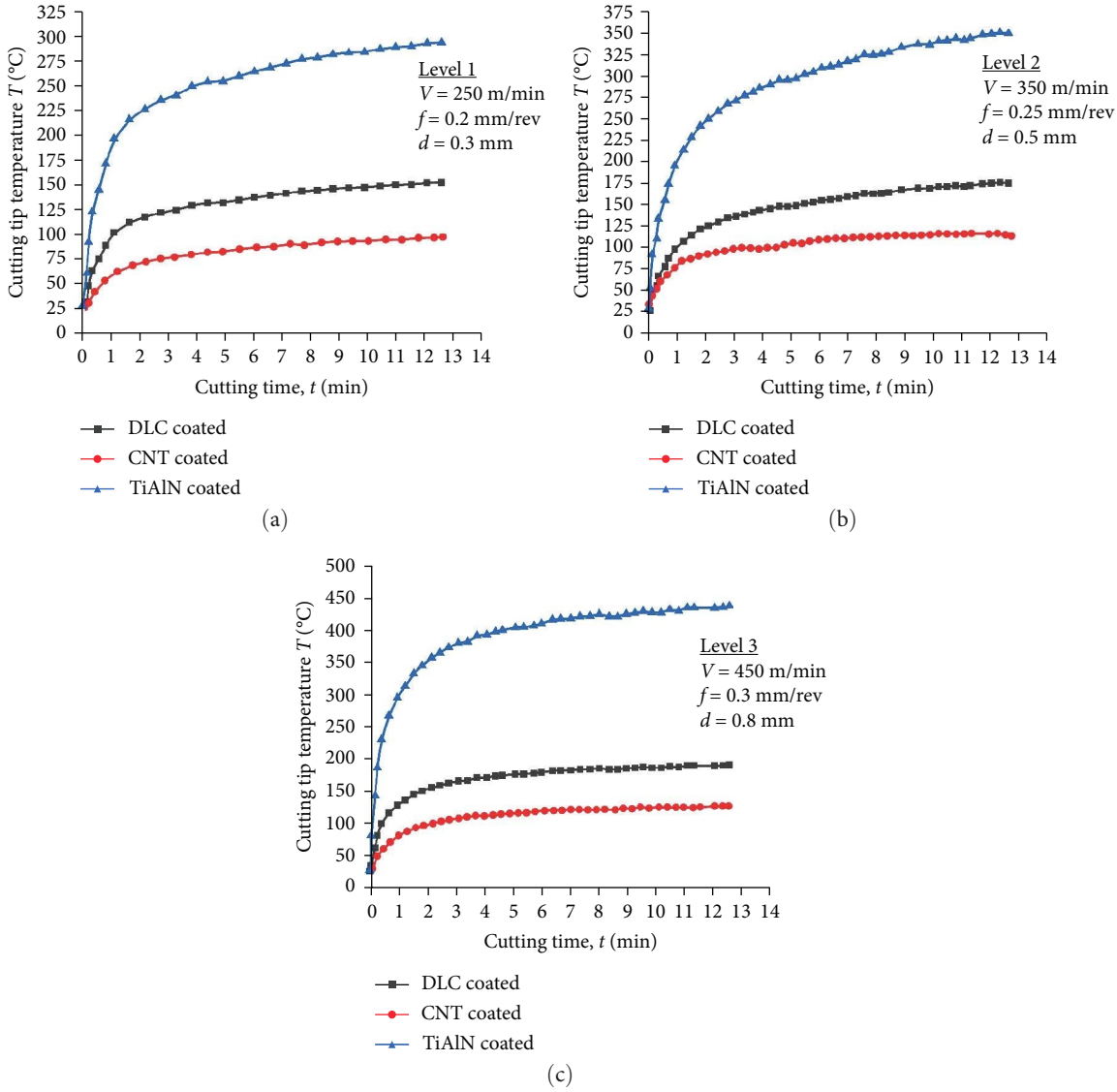

Figure 8: Temperature results at Levels 1, 2, and 3 cutting conditions.

depletion of the tangential forces (F_z) of the CNT-coated tools by a maximum of 50% compared to the TiAlN-coated one and 36% to the DLC-coated one under the extreme cutting environment. The cutting force graphs clearly demonstrate that the TiAlN and DLC-coated tools experience substantial increases in cutting forces at the severe cutting condition compared to the CNT-deposited tool. At the extreme cutting condition, the built-up edge developed over the rake surface due to excess plasticity of the chips, which in turn acts as an obstacle and increases the cutting forces. But the CNT coatings can exhibit excellent lubricity under varied test circumstances [27, 28]. The significant reductions in cutting forces seen with a CNT-coated tool are attributed to the excellent lubricity character of CNT. This phenomenon rewards the development of built-up edge over the rake surface by decelerating the plasticity of the chips. The dynamometer result observed for the DLC-coated tool at Level 1 is shown in Figure 10.

3.5. Chip Morphology. Figures 11–13 show the captured images of the chips produced at the cutting conditions Levels 1, 2, and 3, respectively. The study of the chips reveals a few interesting thermo-mechanical facts. For all machining conditions, the nature of chips produced using the CNT-coated tool does not have much curling effect compared to that TiAlN-coated tool. The heat induced between the workpiece and tool interface was dissipated very rapidly in CNT-coated tools due to the high thermal conductivity of CNT. This phenomenon is attributed to producing the chips with minimum plastic deformations. As the temperature increases, the difference in temperature between the outer and inner sides of the chips also increases, which aggravates the plastic deformation by producing the chips with a more curling effect, as shown in Figures 11(a), 12(a) and 13(a), respectively.

The color of the chips at low-level cutting conditions seems to be golden yellow and turned bluish during the

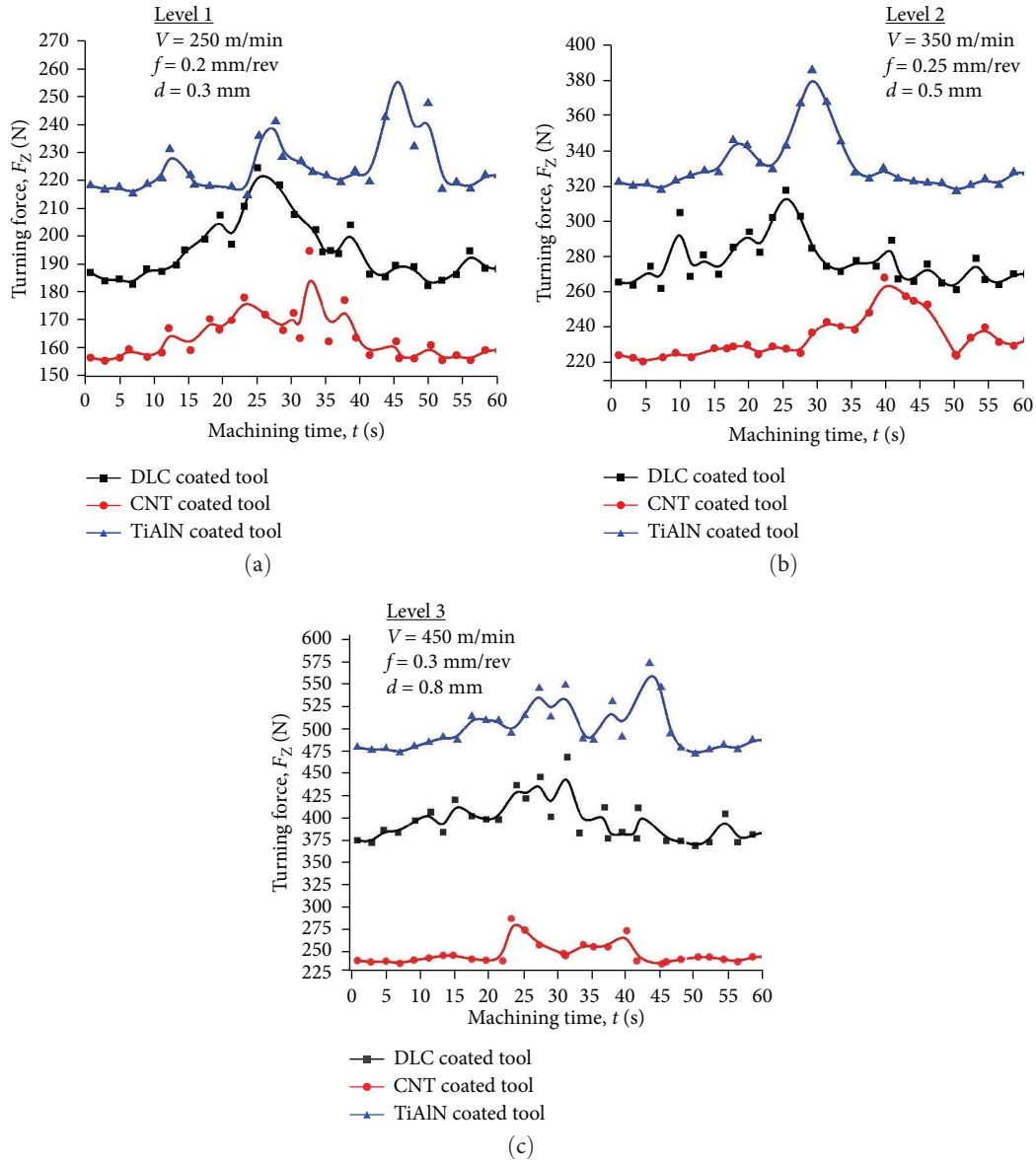

Figure 9: Results of cutting forces at Levels 1, 2, and 3 cutting conditions.

higher cutting conditions. Figure 13(a) confirms that at higher cutting conditions, chips formed with saw tooth edges that abrade on the top of the rake face of the tool, which intensifies the abrasive wear, particularly for the TiAlN-deposited tool. The effect of color and curling is lesser in the chips produced with the CNT-coated tool than TiAlN. The chip morphology study confirms that the development of abrasive wear for CNT-coated tool is significantly lesser than both DLC and TiAlN-coated tools. The chips produced with DLC-coated tool maintain a moderate effect due to its high lubricative surface.

3.6. Wear Mechanisms and Tool Life Analysis. Figure 14(a)–14(c) illustrates the sample images captured through AFM for the TiAlN, DLC, and CNT-coated tools subjected to Level 3 cutting conditions, respectively. The prominence of peaks and valleys in the surfaces observed by AFM images correlates with the damaged tool surface. Indeed, the peaks and valleys recorded by AFM pictures represent the worn-out tool surface. Various studies [48] proved that increasing the cutting speed results in exaggerated peaks and valleys, which indicate tool wear and directly affect the workpiece. In this case, the reduction in the life of the tool can be considered a function of the cutting temperature.

Figure 15 shows the progressions of flank wear for the coated tools under three distinct cutting environments. It is observed that the CNT-coated tools have registered minimal wear compared to the TiAlN and the DLC-coated tools. The comparative findings of flank wear indicate a better reduction in flank wear rates of CNT-coated tools, particularly at higher cutting conditions about 47% and 35%, compared to TiAlN and DLC-coated tools, respectively. The findings

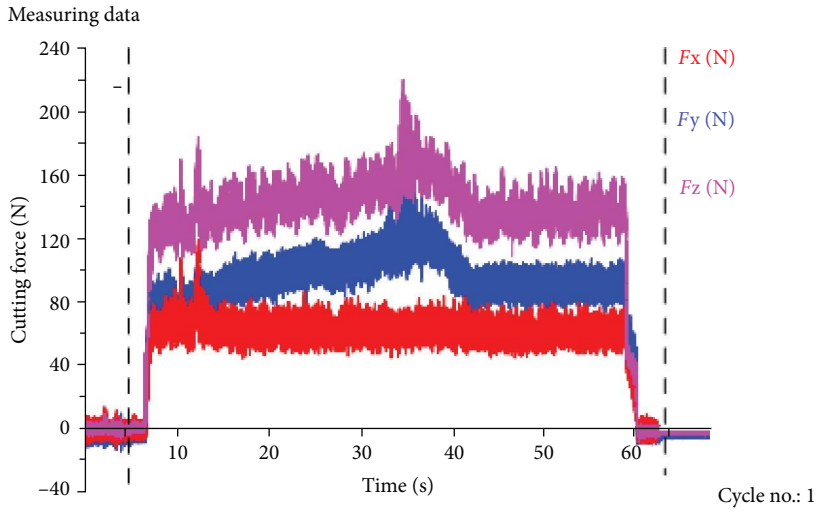

Figure 10: Dynamometer measurement collected during machining with DLC-coated tool at Level 1 cutting condition.

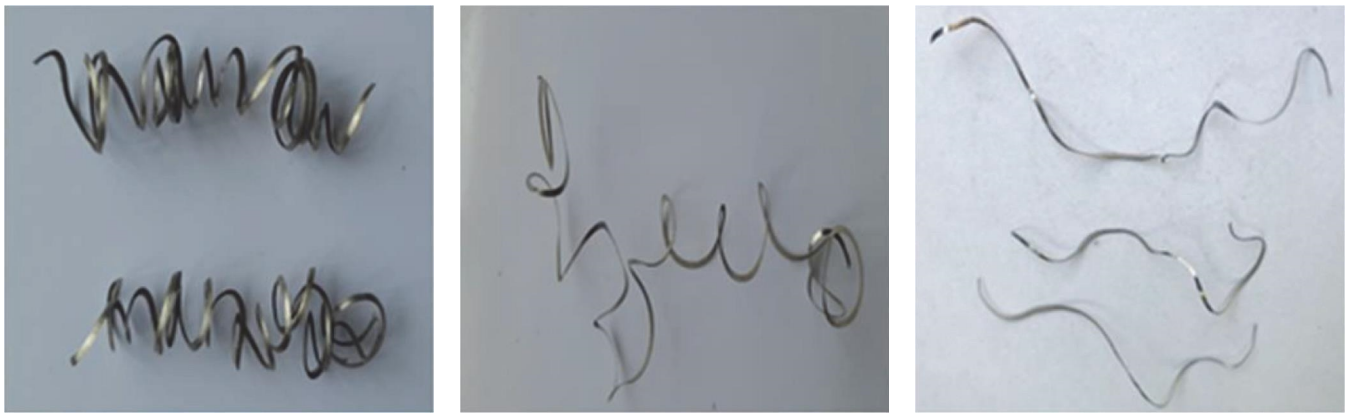

(a) (b) (c)

Figure 11: Chip images at Level 1 cutting condition: (a) TiAlN; (b) DLC; (c) CNT.

(a) (b) (c)

Figure 12: Chip images at Level 2 cutting condition: (a) TiAlN; (b) DLC; (c) CNT.

(a) (b) (c)

Figure 13: Chip images at Level 3 cutting condition: (a) TiAlN; (b) DLC; (c) CNT.

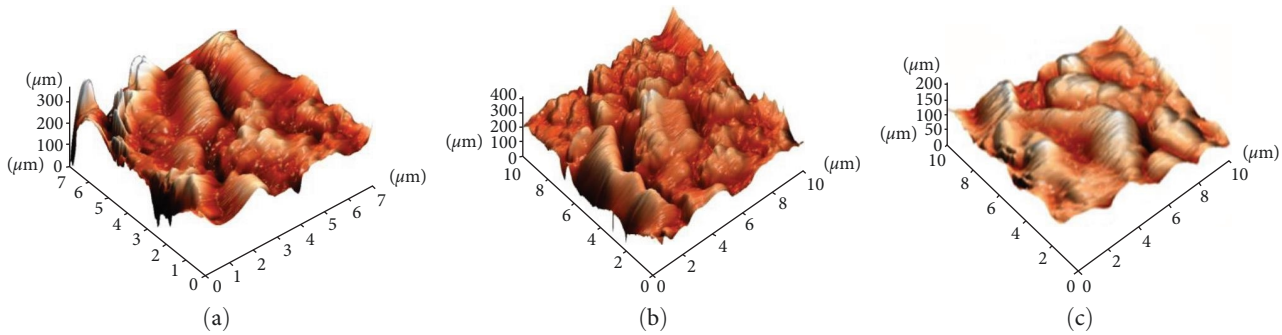

(a) (b) (c)

Figure 14: AFM topographies of flank wear observed for (a) TiAlN; (b) DLC; (c) CNT-coated tools subjected to Level 3 cutting conditions.

showed that the TiAlN-coated tool failed miserably at 47, 39, and 26 min in catastrophic mode under three distinct cutting conditions. At 200°C and above, the wear rate of the DLC film increased dramatically, and further progress at high temperatures led to a complete coating breakdown occurred [49]. Since wear growth is driven by growing cutting parameters, the significant material loss has been observed in the flank portion of the TiAlN-coated tool, as represented in Figure 16(a). Flank wear, coupled with notches, is visible as tiny grooves running parallel to the direction of cutting. Figure 16(a) also depicts the presence of microchipping on the cutting edges. The CNTs improved tribological, thermal, and mechanical properties were attributable to the marginal material loss at the flank face of the CNT-coated tool in extreme cutting conditions, as shown in Figure 16(c).

The comparative tool life in three different cutting conditions for TiAlN, DLC, and CNT-coated tools is shown in Figure 17. The findings show that CNT-deposited tools have an extended tool lives than the TiAlN and the DLC-coated tools of more than 25 and 11 min, respectively, in an extreme cutting environment. In particular, the CNT-deposited tool worked well without noticing significant failure under extreme cutting circumstances (higher cutting speeds and cutting depths).

The nose wear results of the three coated tools are presented in Figure 18. The results show the severe wear growth of the TiAlN-coated tool. During high cutting environments, a tremendous amount of compressive stress and heat were developed, which causes the materials to thermally soften, resulting in plastic deformation of the cutting edges. This huge material loss on TiAlN-coated tool results from the cumulative effect of severe crater wear and plastic deformation at the rake face.

The CNT coating applied over the cutting tool material serves as a thermal shield, which minimizes temperature effects. Moreover, the increased elastic modulus of the CNT enhances resistance to induced compressive stress. The combined impact of minimum cutting tool temperature and compressive stress increases tool life by almost 95% higher than the TiAlN-deposited tool and 27% higher than the DLC-coated one under severe cutting circumstances. Furthermore, the impact of abrasive wear was drastically minimized because of the CNTs incredibly low coefficient of friction and higher thermal conductivity. The greater thermal conductivity characteristic of CNT lowers the amount of heat accumulated in the areas where the tool comes into contact with the workpiece and metal chips. In addition, the antifriction feature of the surface coating is attributed to the reduction of the abrasive action of chips. However, the abrasions of the chips across the TiAlN-coated rake surface at high temperatures result in drastic crater wear.

4. Conclusions

The existence and uniform distribution of CNTs deposited using the PECVD method over the HSS tool substrates was confirmed by Raman spectroscopy and SEM investigations. In addition, the scratch test result reveals that the adhesion

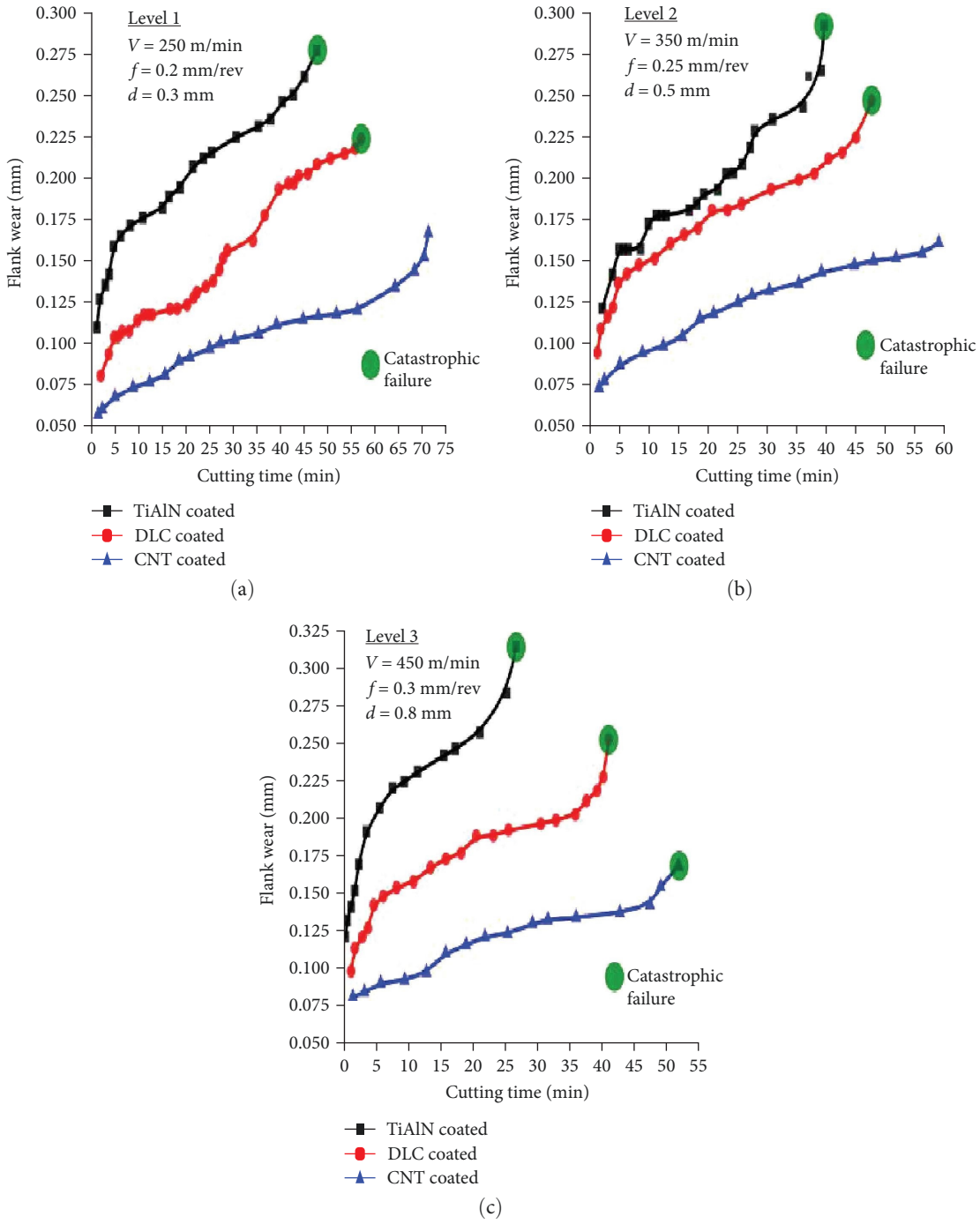

Figure 15: Flank wear progressions of TiAlN, DLC, and CNT-coated tools at Levels 1, 2, and 3 cutting conditions.

strength of CNT coating to the substrate was estimated to be three-fourths of the substrate's yield strength, and the average coefficient of friction of the coated CNT film was 0.075. With the application of the CNT deposition, the cutting temperature was reduced by about 67%–71% compared to the TiAlN-coated tool and by about 33%–36% compared to the DLC-deposited tool. A considerable reduction in tooltip temperature arises from the cumulative impact of the outstanding heat conducting capacity and very low friction coefficient of the CNT-coated tool. Examining major turning forces under various cutting circumstances reveals that CNT-deposited tools reduce cutting forces by 15.5%–36% than DLC-coated tools and by 28%–50% than TiAlN-coated tools. Chip morphology analysis confirms that the shape and color of the chips produced with the CNT-coated tool acknowledge rapid heat dissipation and low abrasion chip wear. The effect of burning color and saw tooth formation with excessive curling for the chip produced with TiAlN and DLC were more severe than CNT. The image of the chips produced at elevated cutting conditions discloses severe wear

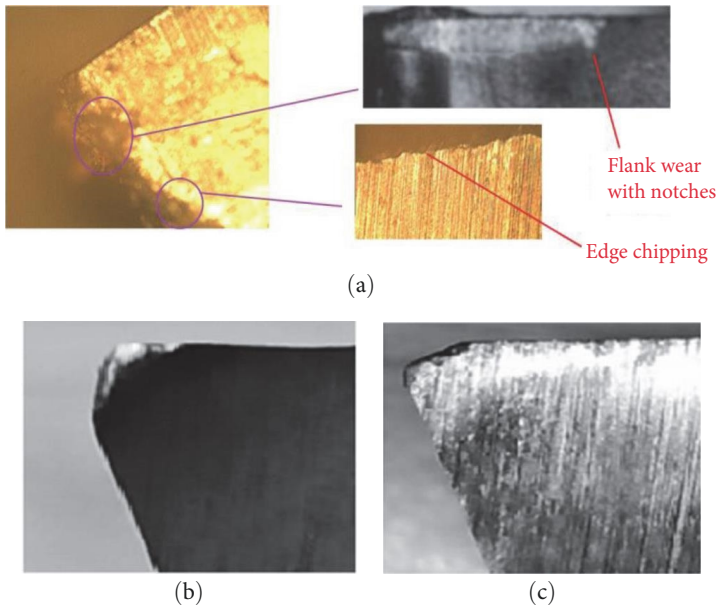

Figure 16: Flank wear of (a) TiAlN; (b) DLC; (c) CNT-coated tools.

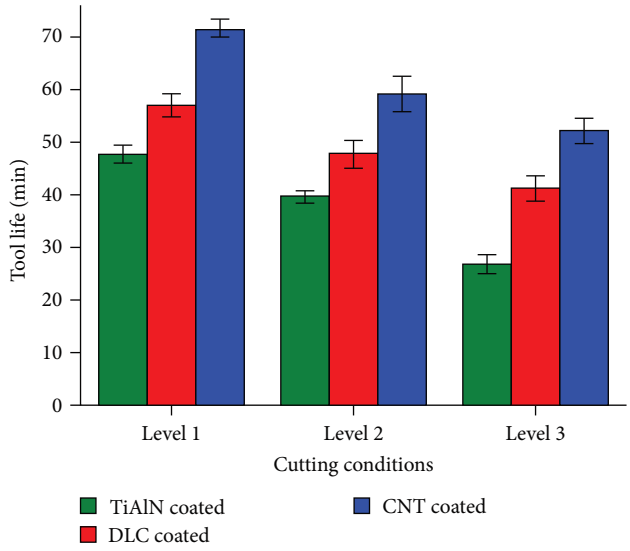

Figure 17: Comparison of the tool life of TiAlN, DLC, and CNT-coated tools under three distinct cutting conditions.

and loss of tool lives for both TiAlN and DLC-coated tools. Under severe cutting conditions, the wear at the flank portion of the CNT-deposited tool was reduced to 34.7% and 46.5%, respectively, compared to DLC and TiAlN-deposited tools. Increasing the cutting parameters of a TiAlN-coated tool led to a significant increase in the flank wear. Followed by this, DLC-coated one showed moderate flank wear. Among the three coated tools, the progression of flank wear was slow and steady in CNT-deposited tool tested under the same conditions. In terms of tool life, the TiAlN-deposited tool failed catastrophically for about 47, 39, and 26 min, respectively, under three distinct cutting circumstances. However, the CNT-deposited tool was not significantly failed under lower cutting conditions, surprisingly noticed that even at elevated cutting conditions, it served for the cutting period of 52 min. Thus, when used under severe cutting circumstances, the CNT-coated tools improve tool lives by about 95% and about 27% compared to TiAlN and DLC-coated tools. Based on these extensive experimental evaluation results, the CNT-coated tool has been identified as an appropriate candidate for turning more difficult-to-cut materials such as titanium alloy.

Data Availability

The data are available upon journal request.

Conflicts of Interest

The authors declare that they have no conflicts of interest.

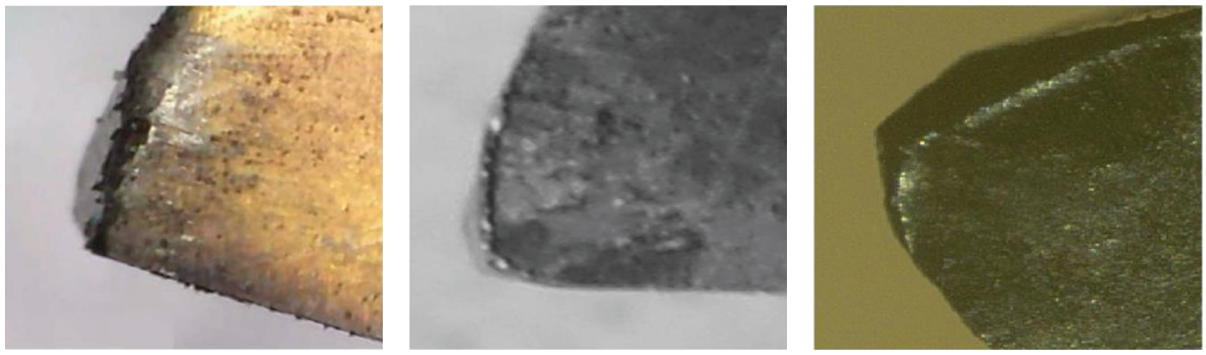

(a) (b) (c)

Figure 18: Nose wear of (a) TiAlN; (b) DLC; (c) CNT-coated cutting tools after turning under Level 3 cutting conditions.

Acknowledgments

The authors extend their appreciation to the Deanship of Scientific Research at King Khalid University, Abha, Asir, Kingdom of Saudi Arabia for funding this work through the Large Groups Project under grant number RGP.2/225/43. The authors would like to thank the Mechanical Engineering Department, Adama Science and Technology University for the support and research facilities.

References

[1] V. Aswinprasad, V. S. Sriharish, C. Venkatesh, A. H. Meda, and N. Kamalakannan, "Experimental investigation of wear characteristics of aluminium 6063 hybrid composite reinforced with graphite and molybdenum disulfide (MoS_2)," *Materials Today: Proceedings*, vol. 22, Part 4, pp. 3190–3196, 2020.

[2] V. Chenrayan, V. Vaishnav, K. Shahapurkar et al., "A comprehensive analysis to assess the impact of nano MoS_2 on the wear characteristic of Al-TiB_2-Gr composite," *Materials Research Express*, vol. 9, no. 1, Article ID 016525, 2022.

[3] V. Vaishnav, R. P. Kumar, and C. Venkatesh, "Influence of nano MoS_2 particle on the mechanical and tribological properties of Al-TiB_2-Gr hybrid composite," *Journal of Mechanical Science and Technology*, vol. 36, pp. 857–867, 2022.

[4] C. Machai and D. Biermann, "Machining of β-titanium-alloy Ti–10V–2Fe–3Al under cryogenic conditions: cooling with carbon dioxide snow," *Journal of Materials Processing Technology*, vol. 211, no. 6, pp. 1175–1183, 2011.

[5] P. V. Badiger, V. Desai, M. R. Ramesh, B. K. Prajwala, and K. Raveendra, "Effect of cutting parameters on tool wear, cutting force and surface roughness in machining of MDN431 alloy using Al and Fe coated tools," *Materials Research Express*, vol. 6, no. 1, Article ID 016401, 2018.

[6] P. V. Badiger, V. Desai, M. R. Ramesh, S. Joladarashi, and H. Gourkar, "Tribological behaviour of monolayer and multilayer Ti-based thin solid films deposited on alloy steel," *Materials Research Express*, vol. 6, no. 2, Article ID 026419, 2019.

[7] P. V. Badiger, V. Desai, M. R. Ramesh, B. K. Prajwala, and K. Raveendra, "Cutting forces, surface roughness and tool wear quality assessment using ANN and PSO approach during machining of MDN431 with TiN/AlN-coated cutting tool," *Arabian Journal for Science and Engineering*, vol. 44, pp. 7465–7477, 2019.

[8] C. Venkatesh, A. S. Karthi, T. Logeswaran, V. Prithivirajan, and M. Santhosh, "Experimental investigation of tribological characteristics of nanocrystalline nickel protective coating developed through electro deposition technique," *Materials Today: Proceedings*, vol. 3, no. 9, pp. 3121–3129, 2016.

[9] P. V. Badiger, V. Desai, and M. R. Ramesh, "Development and characterization of Ti/TiC/TiN coatings by cathodic arc evaporation technique," *Transactions of the Indian Institute of Metals*, vol. 70, pp. 2459–2464, 2017.

[10] C. Venkatesh, N. Sundara Moorthy, R. Venkatesan, and V. Aswinprasad, "Optimization of process parameters of pulsed electro deposition technique for nanocrystalline nickel coating using gray relational analysis (GRA)," *International Journal of Nanoscience*, vol. 17, no. 01n02, Article ID 1760007, 2018.

[11] Y. Isik, "Investigating the machinability of tool steels in turning operations," *Materials and Design*, vol. 28, no. 5, pp. 1417–1424, 2007.

[12] H. Çalişkan, P. Panjan, and S. Paskvale, "Monitoring of wear characteristics of TiN and TiAlN coatings at long sliding distances," *Tribology Transactions*, vol. 57, no. 3, pp. 496–502, 2014.

[13] V. Prabakaran, "Wear mechanism and tool performance of TiAlN coated during machining of AISI410 Steel," *Journal of Bio- and Tribo-Corrosion*, vol. 4, Article ID 65, 2018.

[14] R. R. R. M. Vannan, T. Moorthy, P. Hariharan, and P. Prabhu, "Effect of physical vapor deposited bilayer (AlCrN + TiAlN) coating on high-speed steel single point cutting tool," *Materials and Manufacturing Processes*, vol. 32, no. 4, pp. 373–376, 2017.

[15] L. Aihua, D. Jianxin, C. Haibing, C. Yangyang, and Z. Jun, "Friction and wear properties of TiN, TiAlN, AlTiN and CrAlN PVD nitride coatings," *International Journal of Refractory Metals and Hard Materials*, vol. 31, pp. 82–88, 2012.

[16] K. Bewilogua and D. Hofmann, "History of diamond-like carbon films—from first experiments to worldwide applications," *Surface and Coatings Technology*, vol. 242, pp. 214–225, 2014.

[17] J. Robertson, "Diamond-like amorphous carbon," *Materials Science and Engineering: R: Reports*, vol. 37, no. 4–6, pp. 129–281, 2002.

[18] A. Erdemir and C. Donnet, "Tribology of diamond-like carbon films: recent progress and future prospects," *Journal of Physics D: Applied Physics*, vol. 39, no. 18, Article ID R311, 2006.

[19] G. Yu, Z. Gong, B. Jiang, D. Wang, C. Bai, and J. Zhang, "Superlubricity for hydrogenated diamond like carbon induced by thin MoS_2 and DLC layer in moist air," *Diamond and Related Materials*, vol. 102, Article ID 107668, 2020.

[20] E. L. Dalibon, R. D. Moreira, D. Heim, C. Forsich, and S. P. Brühl, "Soft and thick DLC deposited on AISI 316L stainless steel with nitriding as pre-treatment tested in severe wear conditions," *Diamond and Related Materials*, vol. 106, Article ID 107881, 2020.

[21] C. Chen, W. Tang, X. Li, W. Wang, and C. Xu, "Structure and cutting performance of Ti-DLC films prepared by reactive magnetron sputtering," *Diamond and Related Materials*, vol. 104, Article ID 107735, 2020.

[22] G. R. Dos Santos, D. D. da Costa, F. L. Amorim, and R. D. Torres, "Characterization of DLC thin film and evaluation of machining forces using coated inserts in turning of Al–Si alloys," *Surface and Coatings Technology*, vol. 202, no. 4–7, pp. 1029–1033, 2007.

[23] M. Folea, A. Roman, and N.-B. Lupulescu, "An overview of DLC coatings on cutting tools performance," *Academic Journal of Manufacturing Engineering*, vol. 8, no. 3, pp. 30–36, 2010.

[24] T. Wada, K. Iwamoto, and H. Sugita, "Tool wear of diamond-like carbon-coated high-speed steel with a Cr-based interlayer in cutting of aluminum alloys," *Applied Mechanics and Materials*, vol. 152–154, pp. 74–79, 2012.

[25] M. Monthioux, *Carbon Meta-Nanotubes: Synthesis, Properties and Applications*, John Wiley and Sons, New York, 1st edition, 2011.

[26] D. Kumar, K. Shahapurkar, C. Venkatesh et al., "Influence of graphene nano fillers and carbon nano tubes on the mechanical and thermal properties of hollow glass microsphere epoxy composites," *Processes*, vol. 10, no. 1, Article ID 40, 2022.

[27] W. Zhang, G. Ma, and C. Wu, "Anti-friction, wear-proof and self-lubrication application of carbon nanotubes," *Reviews on Advanced Materials Science*, vol. 36, no. 1, pp. 75–88, 2014.

[28] J. Umeda, B. Fugetsu, E. Nishida, H. Miyaji, and K. Kondoh, "Friction behavior of network-structured CNT coating on pure titanium plate," *Applied Surface Science*, vol. 357, no. Part A, pp. 721–727, 2015.

[29] B. Pazhanivel, T. P. Kumar, and G. Sozhan, "Machinability and scratch wear resistance of carbon-coated WC inserts," *Materials Science and Engineering: B*, vol. 193, pp. 146–152, 2015.

[30] A. Hirata and N. Yoshioka, "Sliding friction properties of carbon nanotube coatings deposited by microwave plasma chemical vapor deposition," *Tribology International*, vol. 37, no. 11, pp. 893–898, 2004.

[31] T. Borkar and S. Harimkar, "Microstructure and wear behaviour of pulse electrodeposited Ni-CNT composite coatings," *Surface Engineering*, vol. 27, no. 7, pp. 524–530, 2013.

[32] J. P. Salvetat, J.-M. Bonard, N. Thomson et al., "Mechanical properties of carbon nanotubes," *Applied Physics A: Materials Science and Processing*, vol. 69, pp. 255–260, 1999.

[33] M. Chandru, V. Selladurai, and C. Venkatesh, "Experimental evaluation of machinability performance of CNT coated HSS tool during turning of titanium alloy," *Journal of Mechanical Science and Technology*, vol. 35, pp. 2141–2150, 2021.

[34] M. Chandru, V. Selladurai, and C. Venkatesh, "Multiobjective performance investigation of CNT coated HSS tool under the response surface methodology platform," *Archives of Metallurgy and Materials*, vol. 66, no. 2, pp. 627–635, 2021.

[35] V. Chenrayan, C. Manivannan, S. Velappan et al., "Experimental assessment on machinability performance of CNT and DLC coated HSS tools for hard turning," *Diamond and Related Materials*, vol. 119, Article ID 108568, 2021.

[36] M. A. Abdulrahaman, O. K. Abubakre, S. A. Abdulkareem, J. O. Tijani, A. Aliyu, and A. S. Afolabi, "Effect of coating mild steel with CNTs on its mechanical properties and corrosion behaviour in acidic medium," *Advances in Natural Sciences: Nanoscience and Nanotechnology*, vol. 8, no. 1, Article ID 015016, 2017.

[37] C. Veiga, J. P. Davim, and A. Loureiro, "Review on machinability of titanium alloys: the process perspective," *Reviews on Advanced Materials Science*, vol. 34, pp. 148–164, 2013.

[38] A. Hosseini and H. Kishawy, "Cutting tool materials and tool wear," in *Machining of Titanium Alloys,* J. P. Davim, Ed., pp. 31–56, Springer, Berlin/Heidelberg, Germany, 2014.

[39] A. Jorio, M. A. Pimenta, A. G. S. Filho, R. Saito, G. Dresselhaus, and M. S. Dresselhaus, "Characterizing carbon nanotube samples with resonance Raman scattering," *New Journal of Physics*, vol. 5, Article ID 139, 2003.

[40] A. Mangione, G. Lanzara, L. Torrisi, and F. Caridi, "Mechanical properties of nanostructured carbon layers grown by CVD and PLD techniques," *Radiation Effects and Defects in Solids*, vol. 165, no. 6–10, pp. 746–753, 2010.

[41] H. Kim, "LLE review quarterly report (January–March 1985). volume 22," Tech. Rep. DOE/DP40200-02, Laboratory for Laser Energetics, University of Rochester, NY, 1985.

[42] W. Y. Liew, J. L. L. Jie, L. Y. Yan, J. Dayou, C. Sipaut, and M. F. B. Madlan, "Frictional and wear behaviour of AlCrN, TiN, TiAlN single-layer coatings, and TiAlN/AlCrN, AlN/TiN nano-multilayer coatings in dry sliding," *Procedia Engineering*, vol. 68, pp. 512–517, 2013.

[43] C. Bauer, H. Leiste, M. Stüber, S. Ulrich, and H. Holleck, "Mechanical properties and performance of magnetron-sputtered graded diamond-like carbon films with and without metal additions," *Diamond and related materials*, vol. 11, no. 3–6, pp. 1139–1142, 2002.

[44] D. P. Monaghan, D. G. Teer, P. A. Logan, I. Efeoglu, and R. D. Arnell, "Deposition of wear resistant coatings based on diamond like carbon by unbalanced magnetron sputtering," *Surface and Coatings Technology*, vol. 60, no. 1–3, pp. 525–530, 1993.

[45] M. Shamsa, W. L. Liu, A. A. Balandin, C. Casiraghi, W. I. Milne, and A. C. Ferrari, "Thermal conductivity of diamond-like carbon films," *Applied Physics Letters*, vol. 89, no. 16, Article ID 161921, 2006.

[46] J. Hone, M. C. Llaguno, M. J. Biercuk et al., "Thermal properties of carbon nanotubes and nanotube-based materials," *Applied Physics A: Materials Science and Processing*, vol. 74, pp. 339–343, 2002.

[47] R. T. Coelho, E.-G. Ng, and M. A. Elbestawi, "Tool wear when turning hardened AISI 4340 with coated PCBN tools using finishing cutting conditions," *International Journal of Machine Tools and Manufacture*, vol. 47, no. 2, pp. 263–272, 2007.

[48] S. Chinchanikar and S. K. Choudhury, "Wear behaviors of single-layer and multi-layer coated carbide inserts in high speed machining of hardened AISI, 4340 steel," *Journal of Mechanical Science and Technology*, vol. 27, pp. 1451–1459, 2013.

[49] G. W. Stachowiak, *Wear: Materials, Mechanisms and Practice*, John Wiley and Sons, New York, 2005.